

# MoveTouch: Robotic Motion Capturing System with Wearable Tactile Display to Achieve Safe HRI

Ali Alabbas<sup>1</sup>, Miguel Altamirano Cabrera<sup>1</sup>, Mohamed Sayed<sup>1</sup>,  
Oussama Alyounes<sup>1</sup>, Qian Liu<sup>2</sup>, and Dzmitry Tsetserukou<sup>1</sup>

<sup>1</sup> Skolkovo Institute of Science and Technology (Skoltech), 121205, Moscow, Russia  
{ali.alabbas, m.altamirano, mohamed.seyed, oussama.alyounes,  
d.tsetserukou}@skoltech.ru

<sup>2</sup> Dalian University of Technology, China, 116024, Dalian City, P.R.C.  
qianliu@dlut.edu.cn

**Abstract.** The collaborative robot market is flourishing as there is a trend towards simplification, modularity, and increased flexibility on the production line. But when humans and robots are collaborating in a shared environment, the safety of humans should be a priority. We introduce a novel wearable robotic system to enhance safety during Human-Robot Interaction (HRI). The proposed wearable robot is designed to hold a fiducial marker and maintain its visibility to the tracking system, which, in turn, localizes the user's hand with good accuracy and low latency and provides haptic feedback on the user's wrist. The haptic feedback guides the user's hand movement during collaborative tasks in order to increase safety and enhance collaboration efficiency. A user study was conducted to assess the recognition and discriminability of ten designed haptic patterns applied to the volar and dorsal parts of the user's wrist. As a result, four patterns with a high recognition rate were chosen to be incorporated into our system. A second experiment was carried out to evaluate the system integration into real-world collaborative tasks.

**Keywords:** Haptic feedback · Human Robot Interaction · Wearable devices.

## 1 Introduction

The number of robots in the industry is increasing globally, reaching over 3.9 million robots in factories in 2022, according to the International Federation of Robotics (IFR) [8]. Robots are considered helpful associates for carrying out repetitive tasks and operating in hazardous environments, while human dexterity can be harnessed in the operation. However, robots are mostly being implemented in the industry as tools, not as companions for humans. To achieve collaboration between humans and robots, the safety of users has to be guaranteed [21].

Haptic feedback is one of the most efficient ways to guarantee safety [18], which is applied in several domains, including medical applications [6], virtual reality [4], and assisting blind people in indoor environments [9]. All these previous studies are concerned with providing haptic feedback to ensure the safety of users during a hazardous scenario and encouraging people to perform an act to avoid dangerous situations.

Tactile feedback improves mutual perception during human-robot collaboration by communicating the robot’s motion intentions and its status to a human worker using hand-worn haptic feedback devices [7]. Several research endeavors have focused on enhancing safety in HRI scenarios through haptic devices [13]. Haptic feedback works as an excellent notification system for humans [20]. Scheggi et al. attempted to use haptic feedback for human navigation with a mobile robot through a vibrotactile bracelet [17].

Tactile feedback can be given to users on different parts of the body, for example, on the forearm [11], [1], [3], or the palm [5]. Evarsson et al. investigated the perceptual vibrotactile thresholds for a range of frequencies on both the inside and outside areas of the wrist, showing that personalized threshold measurements at the actuator locations will be required in order to fine-tune a device for the user [1]. Stanley et al. evaluated ten forms of tactile feedback using five wearable actuators, showing that repeated taps on the subject’s wrist on the side toward which they should turn enhanced the best performance of the subjects [19].

The main focus of this work is to study different haptic patterns on the up (dorsal) and down (volar) parts of the wrist. We also introduce an improved version of our robotic device, dubbed ArUcoGlide that was previously published [2]. We have enhanced the design of the ArUcoGlide making the device smaller in size based on a differential gear train mechanism.

## 2 MoveTouch Motion Capture System

The proposed system consists of the following components:

1. A wearable robot, dubbed MoveTouch, is responsible for both adjusting the orientation of an ArUco marker held at its end-effector and providing haptic feedback to the user. The movable ArUco marker ensures the visibility of the marker to the motion capture system, avoiding any occlusion due to the movement of the user’s hand. The haptic feedback is provided to the user through five vibration motors controlled independently, which are able to generate different patterns. The haptic system acts as a guidance system that tells the user about the optimal movement of his hand during Human’Robot Interaction (HRI) to avoid any collisions.
2. A motion capture (mocap) system consisting of a computer and a single RGB camera that continuously captures a live video stream of the workspace that consists of a collaborative robot UR10 from Universal Robots and the wearable robot.

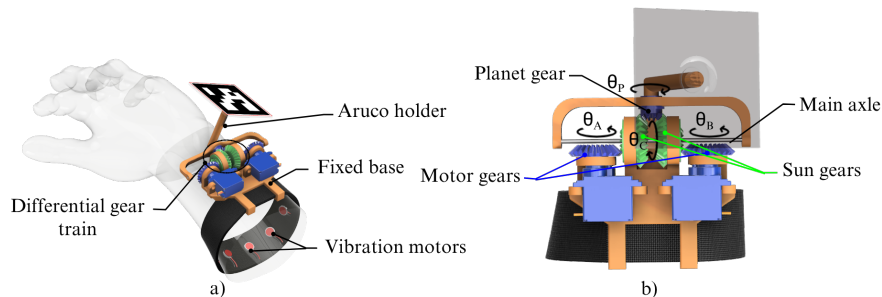


Fig. 1. 3D CAD model of the MoveTouch wearable device.

## 2.1 MoveTouch Wearable Robot

The primary goal of the MoveTouch wearable robot is to assist in determining the user's position and provide vibrotactile guidance, ensuring a secure (HRI) experience.

**Mechanical Design** The proposed device is a two-degrees-of-freedom (2-DoFs) wearable robot, based on a differential gear train mechanism, that holds an ArUco marker at its end-effector with the ability to rotate this marker around two perpendicular axes through two servo motors [10], [12]. Additionally, it includes a bracelet equipped with vibration motors to deliver haptic patterns to the user. The links, holders, and gears were designed and 3D-printed with PLA material; the 3D CAD model is shown in Fig. 1. The device maintains the visibility of the ArUco marker to the tracking system by continuously adjusting the motors' angular position to hold the marker in a fixed orientation to the camera frame.

With the aim of generating two independent motions by means of identical motors placed beside each other, we decided to use a differential gear train mechanism as shown in Fig. 1(a). In this figure, the fixed base, the differential gear train, and the rotating Aruco holder are shown.

We denote  $\Delta\theta_A$  and  $\Delta\theta_B$  as the rotation angles of the first and second motors, respectively. The rotation angles of the ArUco marker around the two axes are  $\Delta\theta_P$  and  $\Delta\theta_C$  which can be seen in Fig. 1(b). The rotations from motors A and B are transmitted to the left and right sun gears of the differential unit. The rotation angles are related by equations:

$$\Delta\theta_A = n_a(n_s\Delta\theta_P + \Delta\theta_C), \quad (1)$$

$$\Delta\theta_B = n_b(n_s\Delta\theta_P - \Delta\theta_C), \quad (2)$$

where  $n_a = n_b = 0.5$  are the gear ratio of the motor gears to the sun gears and  $n_s = 0.5$  is the gear ratio of the sun gears to the planet gear.

We chose to integrate five vibration motors within the system. The selection of this number takes into consideration two key factors: 1) Enabling a uniform distribution of the vibration motors on one side of the user’s wrist (either dorsal or volar), which typically falls within the range of 15-20 cm. 2) This number of vibration motors is sufficient for generating a diverse array of vibrotactile patterns to be employed in user experiments.

**Electronic Design** The electronic parts consist of an ESP32 microcontroller and two Gottech GS-9025MG servo motors that need a supply voltage of 4.8–6 V and give a minimum torque of 2.5 kg.cm. The system is powered by a Li-Po 7.4 V battery connected through a DC/DC converter to power the microcontroller and the servo driver.

Five coin vibration motors, able to vibrate at a frequency in the range 10 to 55 Hz, were located within a distance of 2 cm between them on the bracelet.

The position of the servo motors and the frequency of the vibration motors are controlled via Bluetooth from a base computer.

## 2.2 Motion capture system

To ensure the safety of humans, we need to track the real-time position of the operator within the working space. Our proposed tracking system is both cost-efficient and easy to install, utilizing an ArUco marker to track the operator’s hand. The system comprises a base computer and an HD webcam C930e from Logitech mounted on a stand that can be adjusted to capture different angles of the workspace, providing greater flexibility for the user. The basic idea of the tracking system is to transfer the user’s hand position into the UR10 robot base coordinate system so that we can avoid any collision with it. Since the user’s hand position is known in the camera coordinate system, the transformation from the marker to the camera  $T_C^A$  is known. By attaching another Aruco marker (we will call it the base marker) at a known transformation from the UR10 robot base, we can also get the position of the base of the robot in the camera coordinate system; thus, we can get the transformation  $T_C^B$ . As a result, we obtain the transformation between the user’s hand and the UR10 robot base coordinate system  $T_B^A$ , and thus the position of the user’s hand in the UR10 robot base coordinate system as follows:

$$T_B^A = (T_C^B)^{-1}T_C^A \quad (3)$$

Calculating the transformation from the base marker to the camera  $T_C^B$  is required only once before starting the experiments, as the camera will be in the same position throughout the whole experiment. However, if the camera’s position or orientation is altered, the process needs to be repeated to derive the correct transformation matrix. Once the transformation matrix  $T_C^B$  is determined, we can utilize it to track the position of the ArUco marker that is attached to the user’s hand, enabling us to locate the marker within the UR10 robot’s coordinate system.

### 3 Vibrotactile Guidance System

The proposed wearable device, MoveTouch, provides vibrotactile guidance, facilitating human-robot collaboration. This innovative system harnesses tactile sensations to guide users in adjusting their hand position when the collaborative robot approaches and alerts them about potentially risky situations. To ensure effective information transfer to the user, it's crucial to understand how humans perceive tactile pattern sensations. This perception is achieved through mechanoreceptors, including Merkel cells, Meissner's corpuscles, and Pacinian corpuscles, situated in the outer two layers of the skin—the epidermis and dermis. Merkel cells specialize in sensing sustained pressure and static touch. Meissner's corpuscles are sensitive to low-frequency vibrations within the range of approximately 10 to 50 Hz [14], while Pacinian corpuscles are sensitive to higher-frequency vibrations, typically around 20 to 1000 Hz [15], [16].

#### 3.1 Patterns Design

Given that our wearable robot is worn on the wrist of the user, it is prudent to incorporate vibrotactile patterns in this specific region. We need to first assess the user's ability to recognize vibrotactile patterns on their wrist and determine suitable frequencies for these patterns.

Five different patterns were designed using the five vibration motors, each with two different frequencies. The tactile patterns are illustrated in Fig. 2.

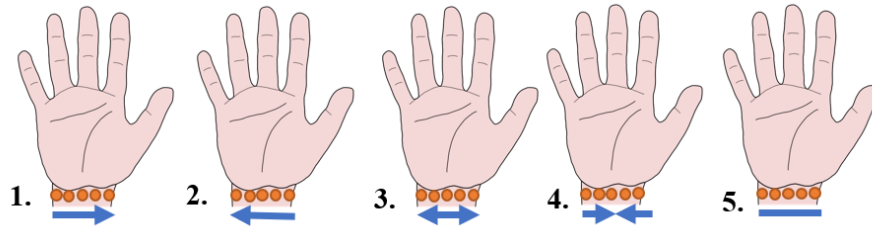


**Fig. 2.** The designed tactile patterns include: 1) Right-to-left propagation; 2) Left-to-right propagation; 3) Center-to-outside propagation; 4) Outside-to-center propagation; and 5) Simultaneous activation of all vibration motors.

As for choosing the frequencies of the patterns, we established two levels: high and low. For the high-frequency patterns, each vibration motor was activated for 0.1 seconds, while for the low-frequency patterns, the activation period for each vibrator was 0.2 seconds. Consequently, the high-frequency rates were 2 Hz for the first and second patterns; 3.3 Hz for the third and fourth patterns; and 10 Hz for the fifth pattern. The corresponding low-frequency rates were 1 Hz

for the first and second patterns, 1.67 Hz for the third and fourth, and 5 Hz for the fifth pattern. We will label each pattern with H or L at the end to mention the frequency (e.g., 1H means the first pattern with a high frequency). The five patterns with two frequencies provide ten different patterns that we will utilize in our study.

In the following subsection, we present an experimental evaluation to assess the pattern recognition of the vibration patterns by users.

### 3.2 Pattern Recognition

In this experiment, we aimed to assess the ability of the participant to recognize and differentiate between the designed vibrotactile patterns. We invited 12 participants and asked them to tell us which haptic pattern they perceived. Their data was recorded and analyzed.

**Subjects** Eleven participants, five women and six men, aged from 23 to 34 years ( $26 \pm 3.05$ ) took part in the experiment. All selected participants were right-handed. The participants were informed about the experiment and filled out the consent form.

**User Study Procedure** Prior to the study, a training session was held to introduce the task, providing users with a detailed explanation of the patterns. Users were asked to wear the MoveTouch robot, and each pattern was rendered three times. A printed piece of paper displaying the patterns was placed in front of the participants throughout the entire training session.

During the study, each user was asked to wear the MoveTouch robot and sit in front of a PC that showed a graphical user interface (GUI) that allowed them to choose the pattern that they felt. An example of the user study of this experiment is shown in Fig. 3.

To identify the optimal wrist location for wearing the device, participants were evaluated twice, wearing the device each time on the upper or lower part of their wrists. The participants were split into two groups: the first group tried the device on the upper part first, followed by the lower part, while the second group followed the opposite sequence. Each of the 10 patterns was replicated five times blindly in a random order; thus, 50 patterns were provided to each participant in each evaluation. Participants were asked to wear headphones while playing white noise and engaged in the experiment through the GUI interface. They had the option to initiate the vibration pattern when they were ready and select from the displayed patterns the one that they felt. During the experiment, participants were not allowed to repeat any pattern.

**Results** The results for each evaluation (dorsal part and volar part) were analyzed and presented in a confusion matrix. In order to evaluate the statistical significance of the differences between the perceptions of the patterns with different frequencies, we analyzed the results using a single-factor repeated-measures

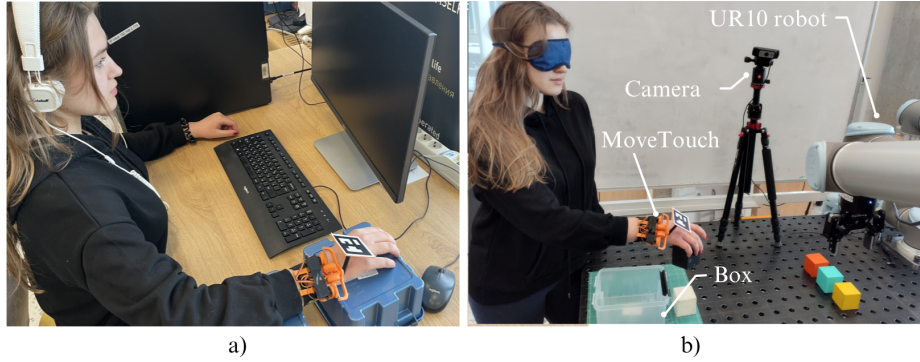


**Fig. 3.** The experimental setup, a) the pattern recognition experiment setup, b) the system evaluation in a real collaborative task setup.

ANOVA, with a chosen significance level of  $\alpha < 0.05$ . The open-source statistical packages Pinguin and Stats models were used for the statistical analysis.

The results of the user perception evaluation by rendering the patterns on the volar part of the wrist are summarized in the confusion matrix (see Table 1).

**Table 1.** Confusion matrix for actual and perceived patterns on the volar (down) part of the wrist

%		<i>Answers (Predicted Class)</i>									
		1H	1L	2H	2L	3H	3L	4H	4L	5H	5L
<i>Patterns</i>	1H	0.80	0.11	0.00	0.00	0.05	0.00	0.02	0.02	0.00	0.00
	1L	0.04	0.96	0.00	0.00	0.00	0.00	0.00	0.00	0.00	0.00
	2H	0.02	0.00	0.69	0.15	0.05	0.02	0.04	0.02	0.00	0.02
	2L	0.00	0.00	0.02	0.98	0.00	0.00	0.00	0.00	0.00	0.00
	3H	0.02	0.00	0.00	0.00	0.38	0.05	0.42	0.07	0.05	0.00
	3L	0.00	0.04	0.00	0.00	0.05	0.82	0.00	0.09	0.00	0.00
	4H	0.07	0.00	0.00	0.00	0.13	0.02	0.64	0.07	0.07	0.00
	4L	0.00	0.00	0.00	0.02	0.00	0.07	0.13	0.78	0.00	0.00
	5H	0.00	0.00	0.00	0.00	0.11	0.00	0.02	0.00	0.82	0.05
	5L	0.02	0.00	0.00	0.00	0.04	0.02	0.04	0.02	0.18	0.69

According to the ANOVA results, there is a statistically significant difference in the recognition rates for the different patterns on the volar part of the wrist:  $F(9, 100) = 5.78, p = 2 \cdot 10^{-6}$ . The ANOVA showed that the patterns and frequencies significantly influenced the perceptions of the users.

The paired t-tests with one-step Bonferroni correction showed statistically significant differences between the patterns 1H and 3H ( $p = 4.95 \cdot 10^{-3} < 0.05$ ), 1L and 3H ( $p = 1 \cdot 10^{-7} < 0.05$ ), 3H and 4L ( $p = 7.3 \cdot 10^{-5} < 0.05$ ), 3H and

5H ( $p = 3.68 \cdot 10^{-2} < 0.05$ ), 2L and 3H ( $p = 1 \cdot 10^{-7} < 0.05$ ), 2L and 4L ( $p = 1.40 \cdot 10^{-2} < 0.05$ ), and 3H and 3L ( $p = 2.24 \cdot 10^{-3} < 0.05$ ).

The results of the human perception evaluation by rendering the patterns on the dorsal part of the wrist are summarized in the second confusion matrix (see Table 2).

**Table 2.** Confusion matrix for actual and perceived patterns on the dorsal (up) part of the wrist

%		<i>Answers (Predicted Class)</i>									
		1H	1L	2H	2L	3H	3L	4H	4L	5H	5L
<i>Patterns</i>	1H	0.87	0.07	0.00	0.00	0.00	0.02	0.02	0.02	0.00	0.00
	1L	0.05	0.95	0.00	0.00	0.00	0.00	0.00	0.00	0.00	0.00
	2H	0.00	0.02	0.76	0.07	0.09	0.02	0.02	0.02	0.00	0.00
	2L	0.00	0.00	0.05	0.95	0.00	0.00	0.00	0.00	0.00	0.00
	3H	0.00	0.00	0.00	0.00	0.45	0.04	0.38	0.04	0.05	0.04
	3L	0.02	0.00	0.00	0.05	0.04	0.71	0.00	0.18	0.00	0.00
	4H	0.05	0.00	0.02	0.00	0.35	0.02	0.42	0.02	0.13	0.00
	4L	0.05	0.02	0.00	0.02	0.05	0.18	0.13	0.49	0.00	0.05
	5H	0.00	0.00	0.00	0.00	0.04	0.00	0.05	0.00	0.78	0.13
	5L	0.00	0.00	0.00	0.00	0.04	0.00	0.04	0.02	0.20	0.71

According to the ANOVA results, there is a statistically significant difference in the recognition rates for the different patterns on the dorsal part of the wrist:  $F(9, 100) = 7.5724$ ,  $p = 2.158 \cdot 10^{-8}$ . The ANOVA showed that the patterns and frequencies significantly influenced the perceptions of the users.

The paired t-tests with one-step Bonferroni correction showed statistically significant differences between the patterns 1H and 3H ( $p = 0.0026 < 0.05$ ), 1H and 4H ( $p = 0.0176 < 0.05$ ), 1H and 4L ( $p = 0.001 < 0.05$ ), 1L and 3H ( $p = 0.0003 < 0.05$ ), 1L and 4H ( $p = 0.003 < 0.05$ ), 1L and 4L ( $p = 8 \cdot 10^{-5} < 0.05$ ), 2L and 3H ( $p = 0.0001 < 0.05$ ), and 2L and 4H ( $p = 0.002 < 0.05$ ).

**Conclusion** The average recognition rate of all patterns on the dorsal part of the wrist was 66.6%, while on the volar side of the wrist, it was 75.64%. We can notice that almost all the patterns are better recognized on the lower part of the wrist; thus, this position of the vibration motors was selected. The patterns that presented a recognition rate higher than 80% were chosen: patterns 1L, 2L, 3L, and 5H will be used for further studies.

### 3.3 System evaluation in real collaborative task

In this evaluation, the system was integrated into a real collaborative task to study its effectiveness in enhancing the overall safety of the user and guiding him to a desired position. The four chosen patterns were integrated to guide the user on how to move his hand as follows: Pattern 1L means to move the hand



to the right, pattern 2L means to move the hand to the left, pattern 3L means to move the hand down, and pattern 5H means to move the hand back.

**Subjects** Eight participants, comprising 5 men and 3 women, were randomly selected from the set of participants who took part in the first experiment.

**Experimental setup** The participants were asked to stand in front of a Siegmund welding table, where a UR10 robot was performing a pick-and-place task of cubes positioned at specific locations on the table. The participants wore the MoveTouch on their right wrist and utilized an eye cover to eliminate any visual feedback about the location of the robot’s Tool Center Point (TCP). Participants were also performing a pick-and-place task in the same box that the robot was using. The surveillance camera was placed on a tripod near the table, where it could monitor the entire workspace. An observer was present during the experiment, poised to activate the emergency button to halt the robot in case of any unforeseen issues. The experimental setup is shown in Fig. 3.

**Collaborative Task Procedure** Before the experiment, every participant underwent a training session covering the four patterns and the corresponding movements associated with each pattern.

The robot picks cubes from certain positions on the table and places them in a box near the participant. The participants were asked to touch and familiarize themselves with the box to memorize its position. Throughout the experiment, participants were asked to pick cubes near the box and place them inside the box. The whole experiment was conducted while the user’s eyes were covered.

During collaboration, when the robot’s TCP is moving towards the participant’s hand and gets to a distance closer than 40 cm (the activation area), the system activates a certain haptic pattern on the participant’s wrist to make participants move their hand in response to each pattern as follows: 1) If pattern 1L is rendered, the participant should move their hand to the left. 2) When the pattern is 2L rendered, the participant should move the hand to the right. 3) For the pattern 3L, the movement should be downward. 4) For pattern 5H, the participant should move the hand backward.

For safety concerns, the robot is forced to stop when its TCP comes within a critical threshold (25 cm) from the participant’s hand and continues to move when the user’s hand gets outside the critical area.

We measured the response time that the participants needed to get their hands out of the dangerous area. The time was measured between the moment the MoveTouch gives the haptic pattern and the moment users start to move their hands. The measured time for all users for each pattern can be seen in Fig. 5. We can see that the mean response times were 0.24 sec, 0.61 sec, 0.85 sec, and 2.41 sec for the first, second, third, and fourth patterns, respectively. We can see that the response time of the fourth pattern is the highest among all the patterns.

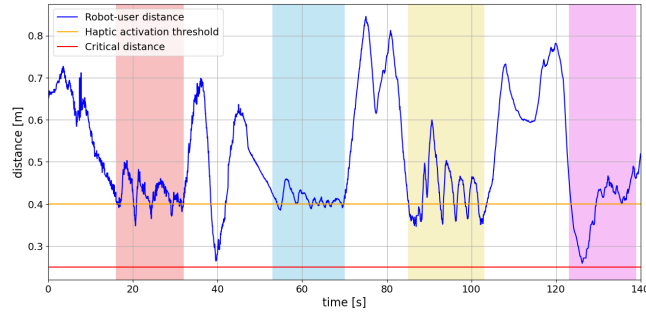


**Fig. 4.** The distance between the participant and the robot’s TCP. The red line is the critical distance, while the orange line represents the haptic activation distance. The four highlighted areas are the areas where the robot is approaching the human.

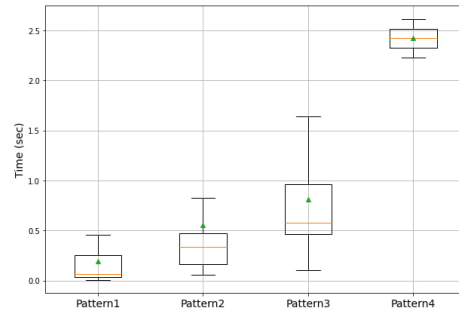


**Fig. 5.** The response time for participants to remove their hands for the four patterns.

**Results** The distance between the participant’s hand and the robot’s TCP is illustrated in Fig. 4. We can observe that the critical distance was preserved throughout the experiment, which indicates safer collaboration, taking into account that the user was doing the task while eye-covered. All participants were able to respond to the haptic patterns correctly, with the exception of one, where the pattern 5H was used to move downward instead of backward. We can see the effective response to the haptic patterns in the highlighted areas in Fig. 4. Those areas correspond to the moment in which the robot is approaching the participant. For example, in the blue highlighted area, the participant is trying to continue the task and return the hand near the box many times, but the robot is still approaching, triggering the haptic pattern multiple times. Consequently, the participant moves their hand again, resulting in this oscillating robot-user distance.

## 4 Conclusion and Future Work

This research presents an innovative wearable robotic system featuring both motion capture and a haptic guidance system designed for human-robot interaction. The system includes a wearable 2-DoFs robot responsible for adjusting a marker, ensuring its constant visibility to the camera. The haptic guidance system incorporates five vibration motors positioned at the user's wrist. A total of ten haptic patterns were selected for experimentation on both the volar and dorsal parts of the wrist. A user study was conducted to evaluate the recognition and discriminability of these patterns. Patterns with the highest recognition rates were subsequently chosen. Another experiment was made to evaluate the integration of the system into a real-world collaborative task. We saw that the critical distance had not been violated during the whole experiment and that the users were efficiently responding to the haptic system.

For the future, we aim to further study the response time of the users for all four patterns and to study how a different application and the speed of the robot might affect the result.

## References

1. Ævarsson, E.A., Ásgeirsdóttir, T., Pind, F., Kristjánsson, Á., Unnthorsson, R.: Vibrotactile threshold measurements at the wrist using parallel vibration actuators. *ACM Transactions on Applied Perceptions (TAP)* 19(3), 1–11 (2022).
2. Alabbas, A., Cabrera, M.A., Alyounes, O., Tsetsrukou, D.: Arucoglide: a novel wearable robot for position tracking and haptic feedback to increase safety during human-robot interaction. In: 2023 IEEE 28th International Conference on Emerging Technologies and Factory Automation (ETFA). pp. 1–8 (2023). <https://doi.org/10.1109/ETFA54631.2023.10275727>
3. Altamirano Cabrera, M., Heredia, J., Tirado, J., Panov, V., Hagos, F., Tsetsrukou, D.: Cohaptics: Development of human-robot collaborative system with forearm-worn haptic display to increase safety in future factories. In: 2021 IEEE 17th International Conference on Automation Science and Engineering (CASE). pp. 74–80 (2021). <https://doi.org/10.1109/CASE49439.2021.9551579>
4. Biswas, S., Visell, Y.: Haptic perception, mechanics, and material technologies for virtual reality. *Advanced Functional Materials* 31(39), 2008186 (2021)
5. Dragusanu, M., Villani, A., Prattichizzo, D., Malvezzi, M.: Design of a wearable haptic device for hand palm cutaneous feedback. *Frontiers in Robotics and AI* 8, 706627 (2021)
6. Enayati, N., De Momi, E., Ferrigno, G.: Haptics in robot-assisted surgery: Challenges and benefits. *IEEE reviews in biomedical engineering* 9, 49–65 (2016)
7. Grushko, S., Vysock'y, A., Heczko, D., Bobovsk'y, Z.: Intuitive spatial tactile feedback for better awareness about robot trajectory during human-robot collaboration. *Sensors* 21(17), 5748 (2021)
8. IFR: World robotics industrial robots 2023, statistics, market analysis, forecasts and case studies, <https://ifr.org>
9. Khusro, S., Shah, B., Khan, I., Rahman, S.: Haptic feedback to assist blind people in indoor environment using vibration patterns. *Sensors* 22(1), 361 (2022)
10. Krainev, A.: Dictionary-reference book on mechanisms. Moscow (1987)

11. Moriyama, T., Kajimoto, H.: Wearable haptic device presenting sensations of fingertips to the forearm. *IEEE Transactions on Haptics* 15(1), 91–96 (2022)
12. Morozov, A., Angeles, J.: The design of an innovative large scale schÖnflies-motion generator. *Proceedings of the Canadian Engineering Education Association* (08 2011). <https://doi.org/10.24908/pceea.v0i0.4013>
13. Pacchierotti, C., Prattichizzo, D.: Cutaneous/tactile haptic feedback in robotic teleoperation: Motivation, survey, and perspectives. *IEEE Transactions on Robotics* (2023)
14. Piccinin, M.A., Miao, J.H., Schwartz, J.: Histology, meissner corpuscle (2018)
15. Quindlen, J.C., Lai, V.K., Barocas, V.H.: Multiscale mechanical model of the pacinian corpuscle shows depth and anisotropy contribute to the receptor’s characteristic response to indentation. *PLoS computational biology* 11(9), e1004370 (2015)
16. Sato, M.: Response of pacinian corpuscles to sinusoidal vibration. *The Journal of physiology* 159(3), 391 (1961)
17. Scheggi, S., Aggravi, M., Morbidi, F., Prattichizzo, D.: Cooperative human-robot haptic navigation. In: 2014 IEEE International Conference on Robotics and Automation (ICRA). pp. 2693–2698 (2014). <https://doi.org/10.1109/ICRA.2014.6907245>
18. Seminara, L., Gastaldo, P., Watt, S.J., Valyear, K.F., Zuher, F., Mastrogiovanni, F.: Active haptic perception in robots: a review. *Frontiers in neurorobotics* 13, 53 (2019)
19. Stanley, A.A., Kuchenbecker, K.J.: Evaluation of tactile feedback methods for wrist rotation guidance. *IEEE Transactions on Haptics* 5(3), 240–251 (2012). <https://doi.org/10.1109/TOH.2012.33>
20. Wang, Y., Millet, B., Smith, J.L.: Designing wearable vibrotactile notifications for information communication. *International Journal of Human-Computer Studies* 89, 24–34 (2016). <https://doi.org/https://doi.org/10.1016/j.ijhcs.2016.01.004>, <https://www.sciencedirect.com/science/article/pii/S1071581916000057>
21. Zacharaki, A., Kostavelis, I., Gasteratos, A., Dokas, I.: Safety bounds in human robot interaction: A survey. *Safety Science* 127, 104667 (2020). <https://doi.org/https://doi.org/10.1016/j.ssci.2020.104667>, <https://www.sciencedirect.com/science/article/pii/S0925753520300643>